Integrated acousto-optic polarization converter in a *ZX*-cut $LiNbO_3$ waveguide superlattice

D. Yudistira,[1,*] D. Janner,[1] S. Benchabane,[2] and V. Pruneri[1,3]

[1]*ICFO-Institut de Ciencies Fotoniques, Mediterranean Technology Park, Castelldefels, Barcelona 08860, Spain*
[2]*Institut FEMTO-ST, CNRS, UMR 6174, Université de Franche-Comté, 25044 Besançon Cedex, France*
[3]*ICREA—Institució Catalana de Recerca i Estudis Avançats, 08010 Barcelona, Spain*
**Corresponding author: didit.yudistira@icfo.es*

Received July 8, 2009; revised August 21, 2009; accepted September 11, 2009;
posted September 17, 2009 (Doc. ID 114028); published October 13, 2009

We report an integrated acousto-optic polarization converter exploiting a novel surface acoustic superlattice (S-ASL) transducer. The S-ASL transducer is made of a *ZX*-cut periodically poled lithium niobate (PPLN) crystal with uniform coplanar electrodes for surface acoustic wave (SAW) generation. For a PPLN period of 20 μm the SAW is excited at an rf of about 190 MHz, while the phase matching occurs at an optical wavelength of around 1456 nm. The measured mode conversion efficiency of 90% at an input rf power of 1 W and the 3 dB optical bandwidth of 2.5 nm confirm the confinement of the SAW between the electrode gap and the constructive interaction along the whole 10 mm electrode length. © 2009 Optical Society of America

OCIS codes: 120.2440, 130.3120, 130.2260, 130.2790, 130.3730, 230.1040.

Acousto-optic (AO) polarization converters are key elements in many photonic applications, such as wavelength division multiplexing (WDM) in optical communication [1], spectral filtering of supercontinuum sources of coherent light [2], acoustic modulation [3], and biomedical sensing applications [4]. A state-of-the-art integrated $LiNbO_3$ based AO polarization converter typically combines an interdigitated transducer (IDT) for surface acoustic wave (SAW) generation and a Ti-indiffused optical waveguide in a single piezoelectric crystal. In addition, the SAW lateral confinement is achieved by Ti indifussion into the cladding regions of the optical waveguide to form a so-called doubly confined structure [5,6]. In this way an acoustic waveguide is formed, which leads to a significant increase in the interaction length and, consequently, to higher device performance. The acoustic waveguide formation requires additional fabrication steps that can be cumbersome and suffers from potential leakage of the optical mode into the Ti-indiffused regions used to confine the SAW. Another potential drawback of this configuration lies in the fact that the optical waveguide is usually covered by the metallic layer of the IDT, thus producing an increase in the optical loss.

It has been shown that an acoustic superlattice (ASL) made of periodically poled lithium niobate (PPLN) can give rise to alternative ways for acoustic wave generation [7,8]. In an ASL structure, the acoustic waves can be launched using uniform electrodes, instead of periodic electrodes, with the latter being the case of IDTs. Domain inversion indeed allows switching the sign—from positive to negative—of all odd rank tensors, particularly of the piezoelectric tensor, from one domain to the next, while keeping all even rank tensors—such as permittivity or elastic constant—unaltered. Therefore, the application of a uniform external electric field to the periodic structure will subject the domain walls to a periodic strain resulting from the periodic change in the piezoelectric coefficient, effectively producing localized acoustic sources, and hence to elastic wave generation [8]. The first $LiNbO_3$ AO device using the ASL has recently been reported employing a bulk acoustic wave, i.e., a longitudinal wave that collinearly interacts with the optical wave [9]. However, to the our knowledge there is no report on the use of SAWs in the ASL for the AO interaction in a waveguide geometry.

In this Letter, we demonstrate a different type of an integrated AO polarization converter based on a surface acoustic superlattice (S-ASL) transducer consisting of an ASL and uniform coplanar electrodes for the SAW generation [10]. In particular, we consider the AO device, making use of collinear waveguide interaction between the SAW and the optical mode. The S-ASL transducer (Fig. 1) is a building block in the proposed AO device, which makes it possible to have the surface region—where the AO interaction occurs—free of any metallic layer, which could induce unwanted optical loss. In addition, the SAW energy is confined in the gap between electrodes, thus avoiding the need for any additional acoustic waveguide. The latter, as was said above, requires additional fabrication steps and might lead to possible detrimental outcoupling of the optical mode.

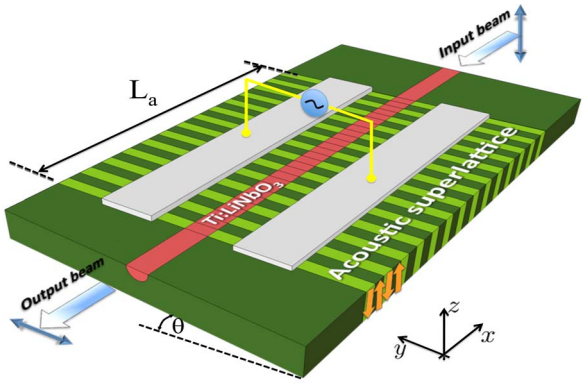

Fig. 1. (Color online) Scheme of the proposed integrated AO polarization converter based on S-ASL on *ZX*-cut PPLN with coplanar uniform electrodes.

The proposed device relies on TE to TM, or vice versa, polarization conversion of optical modes owing to the AO interaction. The SAW induces a periodic stress along the direction of propagation of the optical wave. Through the photoelastic effect, a corresponding periodic rotation of the crystal refractive index ellipsoid occurs, making possible the energy transfer between orthogonally polarized optical modes. The conversion is efficient at the phase-matching condition $\Delta=|\beta_M-\beta_E|-K=0$, with $K=2\pi/\Lambda$ the acoustic wavenumber, Λ the acoustic wavelength, and β_E (β_M) being the propagation constant of the TE (TM) mode. In correspondence to phase matching, we obtain

$$f_a=\frac{V_{\mathrm{SAW}}}{\lambda_0}|N_E-N_M|, \tag{1}$$

where f_a is the phase-matching acoustic frequency, V_{SAW} is the velocity of the SAW, λ_0 is the optical wavelength, and $N_{E(M)}$ is the effective index of the TE (TM) mode. Given the SAW frequency f_a, only optical waves satisfying the condition in Eq. (1) will experience the maximum polarization conversion. For optical wavelengths far from λ_0 the phase-matching condition is no longer satisfied and the conversion efficiency rapidly decreases.

The power conversion efficiency η between TE and TM modes is defined as the ratio of the converted power at $x=L_i$ (L_i is the interaction length) and the input power at $x=0$ [11],

$$\eta=\frac{P_M(x=L_i)}{P_E(x=0)}=\frac{\kappa^2}{\kappa^2+\Delta^2}\sin^2(L_i\sqrt{\kappa^2+\Delta^2}),$$

$$\eta(\Delta=0)=\sin^2(\kappa L_i), \tag{2}$$

where κ denotes the coupling coefficient. As shown in Eq. (2), κ will determine the conversion efficiency of the structure along with the phase mismatch Δ. Moreover, the 3 dB bandwidth of the AO filter is inversely proportional to the interaction length L_i, namely,

$$\Delta\lambda\approx 0.86\frac{\lambda_0^2}{L_i|N_E-N_M|}. \tag{3}$$

As illustrated in Fig. 1, the structure, which is realized on 500-μm-thick z-cut $LiNbO_3$, consists of two main parts, namely, the optical waveguide and the S-ASL transducer. The optical waveguide was fabricated through indiffusion of Ti on the $-z$ face at $T=1060\,^{\circ}\mathrm{C}$ for 7 h. The width and thickness of the Ti film before diffusion were chosen to get a final waveguide width of $W=6$ μm to obtain single-mode propagation at around 1450 nm. The ASL structure was fabricated by an electric-field domain inversion technique [12]. The period of the superlattice (acoustic wavelength) is $\Lambda=20$ μm, which corresponds to the Rayleigh type SAW excitation at a frequency of $f_a=V_{\mathrm{SAW}}/\Lambda=190$ MHz with $V_{\mathrm{SAW}}=3795$ m/s in ZX-$LiNbO_3$. The final ASL structure comprises 500 periods reaching a total length of $L_a=10$ mm. A pair of 200-nm-thick coplanar aluminum electrodes, with a gap of 100 μm and a width of $W=100$ μm, was fabricated by sputtering deposition and subsequent wet etching. The electrodes were aligned parallel to the optical waveguide so that the waveguide remained in the center. The total length of the electrode is taken to be $L_e=L_a=10$ mm. To increase the optical coupling efficiency to the input and output fibers and to avoid backreflection effects of the SAW, the sample's edges were polished at $\theta=8°$.

The experimental characterization setup is shown in Fig. 2. A supercontinuum laser source was used to generate a broad spectrum in the wavelength region of interest and a pigtailing station was used to couple light into and out of the waveguide through a pair of single mode fiber blocks in a butt-coupling configuration. The polarizer (P) and the analyzer (A) were set to be orthogonal to each other and placed before and after the sample. An optical spectrum analyzer (OSA) was used to monitor the optical output, while a network analyzer was used to measure the electroacoustic response. For the acoustic generation, an amplified rf signal generator was employed.

We initially characterized the S-ASL by measuring the scattering parameter $S11$. As shown in the inset of Fig. 3 a strong depth around the resonance frequency of $f_a=189.94$ MHz is obtained, thus demonstrating the SAW generation as expected. The corresponding impedance match of the device around that frequency is measured to be about 65 Ω. After the electroacoustic characterization, we measured the AO response. By keeping P_{rf} constant at 500 mW, the rf f_{rf} was swept around the resonance frequency f_a and the optical output was measured around the phase-matching wavelength of $\lambda=1456$ nm (Fig. 3). The values reported in Fig. 3 are normalized to the peak value at the phase matching ($\Delta=0$). At an rf power (P_{rf}) of 500 mW and a frequency (f_{rf}) equal to f_a (189.94 MHz), the output optical intensity is measured as a function of the wavelength (Fig. 4). The 3 dB optical bandwidth (FWHM) $\Delta\lambda$ is 2.51 nm. From Fig. 3 the acoustic FWHM (Δf) is estimated to be about 310 kHz, which is in good agreement with the theoretical prediction (Δf_{th}) $\Delta f_{\mathrm{th}}=f_a(\Delta\lambda/\lambda)=327$ kHz. From these data and using Eq. (3) we can estimate an interaction length of $L_i=9$ mm, which is very close to the physical electrode length.

The polarization conversion efficiency (η)—i.e., the ratio between converted and transmitted power in the absence of an rf signal—as a function of the rf

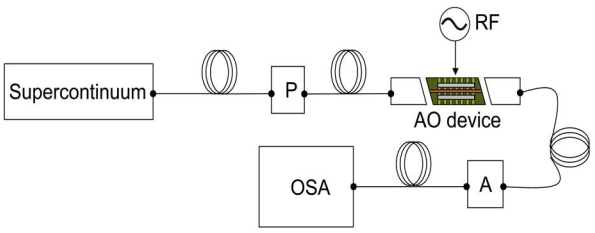

Fig. 2. (Color online) Experimental characterization setup. P and A, polarizer and analyzer, respectively; OSA, optical spectrum analyzer.

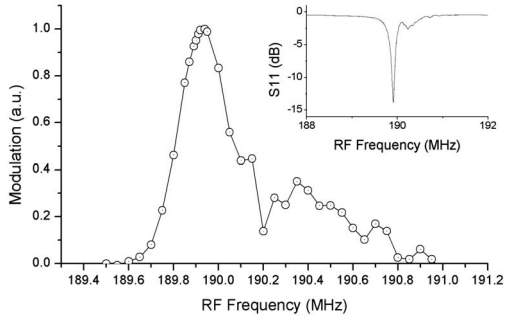

Fig. 3. AO modulation as a function of rf (f_{rf}) at phase matching (around $\lambda = 1456$ nm) for a P_{rf} of 500 mW. In the inset the electroacoustic response of the S-ASL ($S11$ parameter) as a function of f_{rf} is shown.

power is shown in Fig. 5 for values of P_{rf} ranging from 100 to 1600 mW. One can estimate that the 90% conversion is reached for $P_{rf} = 1$ W. This shows that the proposed integrated AO device is significantly more efficient than its bulk counterpart previously reported where, for the same input power, only around 40% mode conversion was achieved [9]. The shift in resonance frequency reported in Fig. 5 for different P_{rf} is mainly due to the thermal drift associated with the rf dissipation, as was already been reported elsewhere, including in [9].

In conclusion, we have presented a monolithic and integrated SAW-based AO polarization converter using a S-ASL transducer. The SAW was excited through the ASL via coplanar electrodes, allowing a metal-free AO waveguide interaction. The TE–TM polarization conversion is achieved through collinear interaction between the generated SAW and the optical waveguide mode. The achieved efficiency and interaction length indicate a strong confinement of the SAW in between the electrodes gap. Further work is required to improve the efficiency of the device in terms of the driving rf power. This would also significantly reduce the heat dissipation and consequently minimize the shift in resonance frequency. The

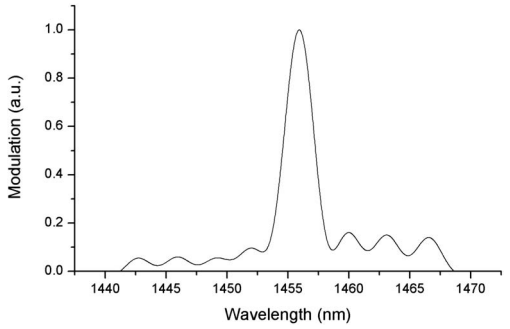

Fig. 4. Optical modulation as a function of wavelength λ for an rf input power of 500 mW and a rf of 189.94 MHz.

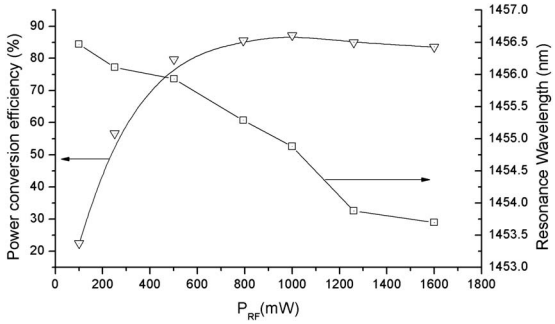

Fig. 5. Power conversion efficiency and resonance wavelength versus rf power.

implementation of the proposed concepts in *ad hoc* designed aperiodic (e.g., chirped) S-ASL can lead to the development of tunable filters, in particular for optical telecommunications, which typically require a tuning range larger than that achieved in this work with uniform periodic ASL.

D. Yudistira and D. Janner acknowledge the support of Generalitat de Catalunya and the Spanish Ministry through a studentship and the Juan De la Cierva fellowship programs, respectively. This work was partially supported by Plan Nacional TEC 2007-60185, Acciones Integradas Hispano-Francesa HF 2008-0033 and by the French Partenariat Hubert Curien (PHC) PICASSO 19220SG. We thank H. Herrmann and W. Sohler for their collaboration.

References

1. M. K. Smith, A. M. J. Koonen, H. Herrmann, and W. Sohler, in *Fiber Optic Communication* (Springer-Verlag, 2001), pp. 262–312.
2. S. K. Dubey, T. Anna, C. Shakher, and D. S. Mehta, Appl. Phys. Lett. **91**, 181106 (2007).
3. T. Xie, Z. Wang, and Y. Pan, Appl. Opt. **44**, 4272 (2005).
4. N. Gupta and R. Dahmani, in *Proceedings of the 19th Annual International Conference of the IEEE Engineering in Medicine and Biology Society* (IEEE, 1997), Vol. 702, p. 702.
5. L. N. Binh and J. Livingstone, IEEE J. Quantum Electron. **16**, 964 (1980).
6. H. Herrmann, P. Muller-Reich, V. Reimann, R. Ricken, H. Seibert, and W. Sohler, Electron. Lett. **28**, 642 (1992).
7. Y.-Q. Lu, Y.-Y. Zhu, Y.-F. Chen, S.-N. Zhu, N.-B. Ming, and Y.-J. Feng, Science **284**, 1822 (1999).
8. Y. Zhu and N. Ming, J. Appl. Phys. **72**, 904 (1992).
9. H. Gnewuch, N. K. Zayer, C. N. Pannell, G. W. Ross, and P. G. R. Smith, Opt. Lett. **25**, 305 (2000).
10. D. Yudistira, S. Benchabane, D. Janner, and V. Pruneri, Appl. Phys. Lett. **95**, 052901 (2009).
11. Y. Ohmachi, J. Appl. Phys. **44**, 3928 (1973).
12. J. Amin, V. Pruneri, J. Webjörn, P. Russell, D. Hanna, and J. Wilkinson, Opt. Commun. **135**, 41 (1997).